The Company of Biologists

RESEARCH ARTICLE

Effects of membrane fatty acid composition on cellular metabolism and oxidative stress in dermal fibroblasts from small and large breed dogs

Ana Gabriela Jimenez[1],[*],[‡], Joshua D. Winward[1],[*], Kenneth E. Walsh[2] and Alex M. Champagne[3]

ABSTRACT

There is ample evidence that cell membrane architecture contributes to metabolism and aging in animals; however, the aspects of this architecture that determine the rate of metabolism and longevity are still being debated. The 'membrane pacemaker' hypothesis of metabolism and of aging, respectively, suggest that increased lipid unsaturation and large amounts of polyunsaturated fatty acids (PUFAs) in cell membranes increase the cellular metabolic rate as well as the vulnerability of the cell to oxidative damage, thus increasing organismal metabolic rate and decreasing longevity. Here, we tested these hypotheses by experimentally altering the membrane fatty acid composition of fibroblast cells derived from small and large breed dogs by incubating them in a medium enriched in the monounsaturated fatty acid (MUFA) oleic acid (OA, 18:1) to decrease the total saturation. We then measured cellular metabolic parameters and correlated these parameters with membrane fatty acid composition and oxidative stress. We found that cells from small dogs and OA-incubated cells had lower maximal oxygen consumption and basal oxygen consumption rates, respectively, which are traits associated with longer lifespans. Furthermore, although we did not find differences in oxidative stress, cells from small dogs and OA-treated cells exhibited reduced ATP coupling efficiency, suggesting that these cells are less prone to producing reactive oxygen species. Membrane fatty acid composition did not differ between cells from large and small dogs, but cells incubated with OA had more monounsaturated fatty acids and a higher number of double bonds overall despite a decrease in PUFAs. Our results suggest that increasing the monounsaturation of dog cell membranes may alter some metabolic parameters linked to increases in longevity.

KEY WORDS: Longevity, PUFA, MUFA, Membrane pacemaker, Primary fibroblasts

INTRODUCTION

That metabolism and longevity are linked to cellular architecture is now becoming a commonly accepted tenet; however, the aspects of this architecture that determine metabolic rate and longevity are still being debated (Hulbert et al., 2007). Cellular membranes, including the plasma and mitochondrial membranes, serve as barriers for the

flow of ions within and between cells, and thus govern the rate of many cellular processes (Hulbert et al., 2007). As a consequence, changes in the properties of these membranes can affect metabolic rate and impact processes associated with aging. A primary mechanism by which membrane properties are altered is through changes in lipid composition, including changes in the saturation of fatty acid tails (Hulbert et al., 2007). Differences in the composition of saturated fatty acids, monounsaturated fatty acids (MUFAs) and polyunsaturated fatty acids (PUFAs) have wide-ranging effects on membrane fluidity and susceptibility to oxidative damage (Calhoon et al., 2015). Currently, two hypotheses attempt to explain the mechanism by which cell membrane composition determines metabolic rate and longevity – the membrane pacemaker hypothesis of metabolism and the membrane pacemaker hypothesis of aging.

The membrane pacemaker hypothesis of metabolism suggests that basal metabolism is closely associated with membrane protein activity such as the pumping of Na^+/K^+-ATPase across the plasma membrane and across the inner mitochondrial membrane (Rolfe and Brown, 1997; Turner et al., 2003). In addition to inherently increasing Na^+/K^+-ATPase activity, lipid membranes with long fatty acid chains and high PUFA content exhibit a greater proportion of more fluid hexagonal phase domains. This greater fluidity increases the activity of several membrane proteins that may increase metabolic rate (Escribá et al., 1995; Brookes et al., 1998; Calhoon et al., 2015). This pattern is demonstrated in a wide range of mammalian species, in which increases in chain length and increases in the total number of double bonds in phospholipids correlate with higher tissue metabolic rates in some organs (Couture and Hulbert, 1995a,b; Hulbert et al., 2007).

In addition to contributing to an elevated metabolic rate, higher levels of unsaturated fatty acids in cell membranes may also increase the susceptibility of the cell membrane to oxidative damage, and thus could lead to an accelerated rate of aging and decreased longevity, a mechanism referred to as the membrane pacemaker hypothesis of aging (Pamplona et al., 1996, 1998, 2002; Portero-Otín et al., 2001; Hulbert et al., 2007; Calhoon et al., 2015). As animals produce adenosine triphosphate (ATP) through mitochondrial respiration, highly reactive molecules with an errant electron known as reactive oxygen/nitrogen species (ROS/RNS) are produced as a by-product of oxygen reduction (Harman, 1956). In small amounts, ROS are important for cell signaling and normal cellular function (Thannickal and Fanburg, 2000). However, when there is an excess of ROS, they interact with other molecules, and can damage cellular components, including lipid membranes (Harman, 1956; Hulbert et al., 2007; Monaghan et al., 2009). As lipid peroxidation propagates across membranes, membrane composition and function are compromised, thus decreasing cellular function. In addition, lipid peroxidation damage initiates a complex chain reaction with highly reactive intermediaries which

[1]Colgate University, Biology Department, 13 Oak Drive, Hamilton, NY 13346, USA. [2]University of Southern Indiana, Chemistry Department, 8600 University Blvd, Evansville, IN 47712, USA. [3]University of Southern Indiana, Biology Department, 8600 University Blvd, Evansville, IN 47712, USA.
*These authors contributed equally to this work

‡Author for correspondence (ajimenez@colgate.edu)

A.G.J., 0000-0001-9586-2866

can propagate excess damage to proteins and DNA (Monaghan et al., 2009). Lipid membranes containing high amounts of PUFAs exhibit the greatest sensitivity to oxidative damage, as PUFAs contain multiple double bonds with an available electron to propagate damage across membranes (Pamplona et al., 1998). It is worth noting, however, that associations between lipid membrane content and longevity may also be explained by the membrane pacemaker hypothesis of metabolism, as metabolism and longevity are correlated in birds and mammals (Hulbert et al., 2007).

To mitigate damage caused by ROS, animals have an endogenous defense system in the form of antioxidants (Harman, 1994). These antioxidants are found in high concentrations in mitochondria, and in lower concentrations throughout the body. Antioxidants such as superoxide dismutase (SOD), catalase (CAT), glutathione peroxidase (GPx), vitamin E and glutathione act by binding to ROS molecules without turning into ROS themselves (Monaghan et al., 2009). Thus, management of ROS and antioxidants becomes a balancing act that must be closely monitored to prevent the pro-oxidant concentration from outweighing the concentration of anti-oxidants sufficient for ROS removal, a process known as oxidative stress (Halliwell and Gutteridge, 2015). Additionally, antioxidant concentration is sometimes related to lipid membrane composition. In some species, higher levels of PUFAs are associated with higher levels of some antioxidants (Yamamoto et al., 2001), and animals may combat high levels of oxidative stress by lowering PUFAs while simultaneously increasing certain antioxidants (Girelli et al., 1992).

Membrane lipid composition is determined by the addition or transfer of fatty acids to phospholipids via deacylation and reacylation cycles (Hulbert et al., 2014). Prior to being added to phospholipids, fatty acids may undergo modifications such as elongation of the hydrocarbon chains or the addition of double bonds regulated by elongase and desaturase enzymes, respectively (Couture and Hulbert, 1995a; Guillou et al., 2010; Pamplona et al., 1998). However, mammals cannot synthesize n-3 and n-6 essential fatty acids, which are the precursors for long-chain polyunsaturated n-3 and n-6 acids; instead, these molecules are obtained from the diet (Pamplona et al., 1998). Therefore, extrinsic modifications to lipid composition can happen through dietary changes or hormone regulation (Couture and Hulbert, 1995a). Caloric restriction experiments have determined that a decrease in cell membrane polyunsaturation is linked to a decrease in lipid peroxidation damage that leads, in some cases, to increased lifespan (Naudí et al., 2013; López-Domínguez et al., 2015). However, cell membrane composition often changes little despite large differences in dietary lipid composition (Abbott et al., 2012), and most changes are limited to the relative percentage of n-6 and n-3 PUFAs (Hulbert et al., 2005; Valencak and Ruf, 2011). Furthermore, concomitant increases or decreases in oxidative stress with changes in membrane saturation and the effects on cellular metabolism and lifespan are not clear. Thus, a direct test of the membrane as a pacemaker hypothesis is still lacking.

Many previous tests of the membrane as a pacemaker hypothesis of metabolism and the membrane as a pacemaker hypothesis of aging are not only limited in their ability to manipulate membrane lipid composition but also often confounded by phylogenetic and body size considerations when comparing multiple species (Speakman, 2005; Calhoon et al., 2015). Here, we tested these hypotheses by measuring cellular metabolism, membrane fatty acid composition and antioxidants in fibroblast cells derived from a wide range of domestic dog breeds, and correlated these traits with lifespan and body size. Domestic dogs are a good study model for

this question because artificial selection has rendered this species with a 44-fold variation in body size from the chihuahua to the Great Dane. Similarly, aging rates are correlated with body size such that small dogs live significantly longer than large dogs (Jimenez, 2016). Furthermore, mammalian fibroblast cells in culture are known to readily take up lipids contained in the culture medium (Glaser et al., 1974; Spector and Yorek, 1985), making them a good model cell type for this experiment. We cultured fibroblast cells of dogs in media enriched with oleic acid, an 18:1 MUFA, to increase the proportion of MUFAs, and decrease PUFA content in cellular membranes. We then measured the effects of this altered membrane composition on cellular metabolism and oxidative stress. Overall, we predicted that a lesser degree of polyunsaturation in membrane fatty acids would result in a decrease in cellular metabolism, and a decrease in oxidative stress in cells from small and large breed dogs. We expected to see a more inflated response in cells from large breed dogs. To our knowledge, this is the first time that cell membrane lipids have been quantified intraspecifically across a large range of dog breeds, and the first time there has been a direct measurement of cellular metabolism and changes in cell membrane composition.

MATERIALS AND METHODS
Advantages of using fibroblast cells
Some advantages to using fibroblasts to address our query include the ability to culture cells from relatively non-invasive procedures, control of environmental nutrients and the ability to measure multiple physiological parameters in the same cell lines (for example, cellular metabolic rate and oxidative stress). Others have demonstrated that there is a relationship between fibroblast membrane lipid composition, longevity and metabolic rate in birds (Calhoon et al., 2014). Though the membrane as a pacemaker hypothesis was postulated for mitochondrial membranes, we measured total phospholipids in whole cells because in mammals, allometric variation in fatty acyl composition is similar for all subcellular compartments and the total fraction of phospholipids has been used as a proxy for variation in mitochondrial membrane composition (Hulbert et al., 2002; Turner et al., 2005).

Isolation of dog fibroblasts
We isolated fibroblast cells from puppies of two size classes. The small breed size class was composed of breeds with an adult body mass of 15 kg or less, and the large breed size class included breeds or mixes with an adult body mass of 20 kg or more (Table 1). These size classes are based on American Kennel Club (AKC) standards of each breed, and are described in Jimenez (2016). Puppy samples were obtained from routine tail docks, ear clips and dewclaw removals performed at veterinarian offices in Central New York and Michigan. The samples were placed in cold transfer medium [Dulbecco's modified Eagle's medium (DMEM) with 4.5 g l^{-1} glucose, sodium pyruvate and 4 mmol l^{-1} L-glutamine supplemented with 10% heat-inactivated fetal bovine serum and antibiotics (100 U ml^{-1} penicillin–streptomycin), containing 10 mmol l^{-1} Hepes] and transferred to Colgate University. To isolate fibroblast cells, skin samples were sterilized in 70% ethanol and 20% bleach. Once any fat and bone had been removed, skin was minced and incubated in sterile 0.5% Collagenase Type 2 (Worthington Chemicals, cat. no. LS004176) overnight in an atmosphere of 37°C, 5% CO_2 and 5% O_2. After incubation, the collagenase mixture was filtered through a 20 µm sterile mesh, and centrifuged at 1000 rpm for 5 min. The resulting supernatant was removed, and the pellet was resuspended with 7 ml of mammal

Table 1. Breeds, sample sizes, adult body mass, mean breed lifespan and range of COV across variables of each breed included in the present study

Breed	Size class	N	Adult body mass (kg)	Mean breed lifespan (years)	COV range for all control variables	COV range for all OA variables
Airedale	Large	5	27.21	9.81	0.3–0.78	0.26–1.41
Boxer/pit bull terrier mix	Large	3	38.92	8.89	0.017–1.01	0.08–1.1
Boxer	Large	7	32.88	8.89	0.36–1.28	0.37–1.46
Cane corso/Rottweiler	Large	1	46.88	9.9	N/A	N/A
Doberman	Large	4	36.28	9.36	0.60–1.29	0.43–1.07
English mastiff	Large	3	79.38	6.9	0.18–0.7	0.23–0.86
Great Dane	Large	5	71.44	7.8	0.36–0.94	0.36–0.96
German short haired pointer	Large	5	26	10.25	0.32–1	0.23–1
German wire haired pointer	Large	5	29.5	8.8	0.32–0.87	0.7–1.4
Labrador retriever	Large	5	30.5	10.7	0.58–1.82	0.61–1.57
Labradoodle	Large	5	26.1	13	0.16–1.33	0.32–1.14
Old English sheep dog	Large	4	36	10	0.37–1.15	0.47–1
Rottweiler	Large	8	48.76	8.87	0.47–1.32	0.41–0.94
Standard poodle	Large	5	26.1	9.6	0.33–1.19	0.36–1.24
Bracco Italiano	Large	1	32.5	12.5	N/A	N/A
Cane corso	Large	4	45	11	0.32–0.92	0.26–1.14
Large Münsterländer	Large	5	27.5	9.04	0.06–0.72	0.17–0.66
King Charles cavalier	Small	5	7	10	0.15–1.17	0.15–0.9
Chihuahua	Small	4	2.2	11.5	0.37–1.21	0.22–0.97
Corgi	Small	6	12	10.29	0.44–1.11	0.35–1.21
Miniature poodle	Small	3	9.1	10.2	0.29–0.67	0.15–0.83
Miniature schnauzer	Small	2	7.25	8.9	0.05–0.9	0.15–0.88
Pomeranian	Small	2	2.7	8.9	0.08–0.81	0.09–0.91
Soft coated wheaten terrier	Small	5	14	8.75	0.7–1.49	0.29–1.54
Toy poodle	Small	6	3.4	12.36	0.44–1.08	0.47–1.55
Yorkshire terrier	Small	5	2.5	10.9	0.46–0.99	0.40–0.98
Havanese	Small	1	5.8	11.1	N/A	N/A

Our study included data from primary fibroblast cells obtained from 17 breeds/mixes of large-sized puppies and 10 breeds/mixes of small-sized puppies, totaling 114 dogs sampled. Breed lifespan data are from Jimenez (2016). OA, oleic acid; COV, coefficient of variation.

media [DMEM with 4.5 g l^{-1} glucose, sodium pyruvate and 4 mmol l^{-1} L-glutamine supplemented with 10% heat-inactivated fetal bovine serum and antibiotics (100 U ml^{-1} penicillin–streptomycin)]. Cells were grown in corning T-25 culture flasks at 37°C in an atmosphere of 5% CO$_2$ and 5% O$_2$. When cells reached 90% confluence, they were trypsinized (0.25%) and cryopreserved at 10^6 cells ml^{-1} in DMEM supplemented with 40% fetal bovine serum and dimethylsulfoxide (DMSO) at a final concentration of 10%. We stored cells in liquid N$_2$ prior to any experiments.

Treatments
For each individual dog, we split cell lines into a control (normal mammal media as listed above) and a treatment (oleic acid, OA) group as follows. Resuspended cells at passage 1 (P1) were given 5 days to recover from freezing before passaging to P2. At P2, each sample was trypsinized again and evenly split in two; 0.25 ml of each sample was added to two T25 culture flasks; 5 ml of DMEM was added to one flask to serve as the control, and 5 ml of 5 mmol l^{-1} OA media was added to the second flask to serve as the experimental treatment. A 50 mmol l^{-1} solution of OA was prepared by making a 10% solution of bovine serum albumin (BSA), and a solution of OA by dissolving 14.1235 g of OA into 1 liter of 0.1 mol l^{-1} NaOH while heating. We used a final 5 mmol l^{-1} concentration of OA in DMEM media for our treatment group (Pappas et al., 2002). The cells were then allowed to grow to confluence at 37°C in an atmosphere of 5% CO$_2$ and 5% O$_2$. All measurements were conducted using cells at P3. All the procedures within this study were approved by Colgate University's Institutional Care and Use Committee. It should be noted that OA at high concentrations has demonstrated toxicity in immune system cells such as lymphocytes (Cury-Boaventura et al., 2006) and in hen egg white lysozomes (Huang et al., 2019). However, to our knowledge, the toxicity of OA has not been demonstrated in dermal fibroblasts and we base our experimental design on studies that have previously used this concentration of OA in human dermal cells (Pappas et al., 2002).

Oxygen consumption rate (OCR) in fibroblast cells
Assays were performed prior to experiments to determine optimal cell seeding density, and optimal concentrations of each compound. We seeded 20,000 cells per well in duplicate per individual into XF-96 cell culture plates and allowed cells to attach overnight. OCR was determined using XF-96 FluxPaks (Agilent Technologies). We measured OCR after cells had equilibrated to running media (10 mmol l^{-1} glucose, 1 mmol l^{-1} sodium pyruvate and 2 mmol l^{-1} glutamine, pH 7.4) for 1 h. Baseline measurements of OCR were made three times to establish basal OCR prior to injecting a final well concentration of 2 μmol l^{-1} oligomycin, which inhibits ATP synthesis by blocking the proton channel of the F$_o$ portion of the ATP synthase, causing OCR to fall. Thus, the decrease in OCR from basal levels represents ATP-coupled respiration, whereas the remaining OCR is attributed to O$_2$ consumption required to overcome the natural proton leak across the inner mitochondrial membrane plus any non-mitochondrial O$_2$ consumption. We then injected a well concentration of 0.125 μmol l^{-1} carbonyl cyanide-4-(trifluoromethoxy)phenylhydrazone (FCCP), an uncoupling agent that disrupts ATP synthesis by collapsing the proton gradient across the mitochondrial membrane, leading to uncoupled consumption of energy and O$_2$ without generating ATP, providing a theoretical maximal OCR. Finally, we injected a final well concentration of

$0.5\ \mu mol\ l^{-1}$ antimycin A, a complex III inhibitor, and rotenone, a complex I inhibitor. This combination stops mitochondrial respiration and enables non-mitochondrial respiration to be evaluated (Gerenser et al., 2009; Brand and Nicholls, 2011; Hill et al., 2012). After measurements were completed, we used a Countess II FL cell counter to count the actual final concentration of cells in each well and normalized all rates to 20,000 cells. In addition to the OCR parameters we measured directly (above), we also calculated spare respiratory capacity as the difference between maximal OCR and basal OCR, and ATP coupling efficiency as the percentage of basal OCR accounted for by ATP-coupled respiration. For each OCR parameter, we followed equations supplied by Divakaruni et al. (2014). Though all cells were actively dividing, because of differing growth rates of each cell line, cells were counted after each experiment using a Countess II FL cell counter and data were normalized to a total of 20,000 cells per well.

Oxidative stress measurements in fibroblast cells
For oxidative stress measurements, cells were seeded at 10,000 cells per well and allowed to attach for 24 h prior to any experiments. We used Thermo Scientific™ Nunc™ MicroWell™ 96-Well Optical-bottom black chimney plates with polymer base (cat. no. 152028) for all fluorescent stains. After staining with each fluorescent stain (below) on a separate plate, cells were imaged using a Tecan Infinite M200 fluorescence microplate reader. Cells were counted after each experiment using a Countess II FL cell counter and data were normalized to a total of 20,000 cells per well.

Reduced glutathione
ThiolTracker™ Violet Kit (Glutathione Detection Reagent, Molecular Probes®) was used to measure concentration of reduced glutathione (GSH). In brief, cells were rinsed with sterile PBS twice and $20\ \mu mol\ l^{-1}$ ThiolTracker was added to each well. Plates were incubated at 37°C, 5% CO_2 and 5% O_2 for 30 min. Cells were then washed another three times with sterile PBS, and imaged in phenol red-free FluoroBrite DMEM. Excitation and emission were measured in the violet spectrum at 404 nm and 526 nm, respectively (Mandavilli and Janes, 2010; Roberts et al., 2017).

ROS production
CellROX® Oxidative Stress Reagents kit (Molecular Probes®) was used to measure ROS production. CellROX reagent was added directly to the serum-free medium at a concentration of $5\ \mu mol\ l^{-1}$ and cells were incubated at 37°C, 5% CO_2 and 5% O_2 for 30 min. Cells were then washed three times with sterile PBS, and imaged in phenol red-free FluoroBrite DMEM. Excitation and emission were in the green spectrum at 488 nm and 530 nm, respectively (Gebhard et al., 2013; Choi et al., 2015). As a positive control, cells were treated with or without $100\ \mu mol\ l^{-1}$ menadione (Sigma cat. no. M5625) prior to being stained with CellROX; this confirmed that the signal was due to ROS production.

Lipid peroxidation damage
Lipid peroxidation (LPO) damage was measured with the Image-iT® Lipid Peroxidation Kit based on the BODIPY® 581/591 reagent. The ratio between red and green indicates the degree of LPO. Cells were stained with $10\ \mu mol\ l^{-1}$ component A and incubated at 37°C, 5% CO_2 and 5% O_2 for 30 min. Cells were then washed three times with sterile PBS and imaged in phenol red-free FluoroBrite DMEM. LPO damage red excitation and emission were measured at 575 nm and 610 nm, respectively, and LPO damage green excitation and emission were measured at 488 nm and

525 nm, respectively (Leirós et al., 2014; Dezest et al., 2017). A final concentration of $100\ \mu mol\ l^{-1}$ cumene hydroperoxide was used as a positive control to induce lipid peroxidation.

Quantifying lipids in fibroblast cell extracts
We used a modified Bligh and Dyer (1959) method to extract lipids from control and OA-incubated cells of each individual dog. Briefly, we suspended cells in 1 ml of sterile, distilled H_2O, and sequentially added 3.75 ml of 1:2 (v/v) chloroform:methanol, 1.25 ml of chloroform and 1.25 ml of $1\ mol\ l^{-1}$ NaCl, vortexing after adding each solvent. We then centrifuged the entire solution at 1000 rpm for 5 min at room temperature to separate aqueous and organic constituents, and recovered the lipids in the organic phase. We then added another 1.88 ml of chloroform to the remaining aqueous phase, centrifuged again, and combined the recovered organic phase with the first organic phase before discarding the aqueous phase. To prepare lipids for gas chromatography (GC), we methylated fatty acid chains via transesterification to produce fatty acid methyl esters (FAMEs). FAMEs were produced by heating the lipid extracts in 2.0 ml of anhydrous methanolic HCl (5%) for 90 min. After cooling, the resultant FAMEs were extracted by adding 1 ml of hexane and 1 ml distilled H_2O (Ichihara and Fukubayashi, 2010). The hexane layer containing the FAMEs was recovered and evaporated, and we redissolved FAMEs in 20 µl 2:1 chloroform:methanol containing $50\ mg\ l^{-1}$ butylated hydroxytoluene as an antioxidant.

We separated FAMEs on a HP 5890A gas chromatograph with flame ionization detector (FID) equipped with a DB-23 column (30 m, 0.25 mm i.d., 0.25 µm film thickness, Agilent Technologies). The oven was programmed to increase from an initial temperature of 50°C to 194°C at a rate of $25°C\ min^{-1}$, held for 1 min, followed by heating at $5°C\ min^{-1}$ to 245°C and holding for 3 min for a total run time of 20.5 min. A volume of 1 µl of the FAME solution was injected with a split ratio of 50:1 (injector temperature, 250°C). Helium was used as the carrier gas at $1.0\ ml\ min^{-1}$ constant flow. Detector conditions were $40\ ml\ min^{-1}$ hydrogen, $400\ ml\ min^{-1}$ air and make up gas $25\ ml\ min^{-1}$ and the temperature was 280°C (Zou and Wu, 2018). Identification of fatty acids was achieved by comparison of retention times with the Supelco 37 standard component FAME mix (CRM47885) and authentic individual FAME standards (MilliporeSigma, St Louis, MO, USA). We used the peak analyzer function of OriginPro19 (OriginLab Corporation, Northampton, MA, USA) to identify each fatty acid and calculate peak areas on each chromatogram. The area of each peak was divided by the sum of the peak area to express each fatty acid as the mol % of total fatty acids.

Statistics
To analyze fatty acid composition, we calculated average chain length, double bond index, peroxidizability index, percentage PUFA, percentage MUFA, percentage saturated fatty acids, percentage PUFAn3 and percentage PUFAn6 (Pamplona et al., 1998). Because these variables were not normally distributed, we transformed the variables with a two-step procedure (Templeton, 2011), and then used paired t-tests to compare control individuals with the same individuals treated with OA. To determine whether fatty acid composition correlates with lifespan, we ran Pearson correlations for each variable in the control group against lifespan. Finally, we used independent sample t-tests to compare fatty acid composition in large and small breeds from the control group. We applied a Bonferroni correction in all instances where multiple independent comparisons were made. All measures of fatty acid composition were analyzed with SPSS 24.0.

Table 2. Mole percentages of membrane fatty acids and parameters derived from these measurements in control cells and cells incubated with OA

Fatty acid	Control (mol %)	OA (mol %)	Significance
16:0	29.78±0.72	22.11±0.70	<0.001
16:1	2.90±0.13	1.43±0.07	<0.001
18:0	27.23±0.68	17.68±0.61	<0.001
18:1	18.87±0.72	40.05±0.96	<0.001
18:2	1.39±0.05	0.94±0.04	<0.001
18:3	0.76±0.11	0.50±0.06	0.748
20:0	1.04±0.15	0.56±0.10	0.004
20:1	0.63±0.03	1.78±0.07	<0.001
20:2	1.98±0.14	2.57±0.12	<0.001
20:3	1.02±0.05	0.81±0.03	0.001
20:4	5.03±0.23	3.67±0.13	<0.001
20:5	0.08±0.01	0.07±0.01	0.579
22:0	1.53±0.16	0.72±0.07	<0.001
22:1	0.54±0.04	0.87±0.04	<0.001
22:2	0.19±0.06	0.06±0.02	<0.001
22:6	2.08±0.10	1.52±0.07	<0.001
24:0	2.01±0.14	0.89±0.06	<0.001
24:1	2.94±0.16	3.77±0.20	<0.001
Lipid parameter			
Average chain length	18.01±0.03	18.13±0.03	0.012
Double bond index	71.31±1.86	83.13±1.70	<0.001
Peroxidizability	50.80±1.76	45.45±1.17	0.014
% Saturated	61.60±1.01	41.96±1.19	<0.001
% MUFA	25.88±0.94	47.90±1.07	<0.001
% PUFA	12.52±0.41	10.14±0.27	<0.001
% PUFA n-3	2.16±0.11	1.60±0.07	<0.001
% PUFA n-6	10.36±0.34	8.54±0.22	<0.001

Values represent means±s.e.m. for all individuals for which pairwise comparisons were available between treatments (n=112). MUFA, monounsaturated fatty acid; PUFA, polyunsaturated fatty acid.

Data from each metabolic and oxidative stress assay were first analyzed for normality using a Shapiro–Wilk test. None of our variables were normally distributed and they did not re-gain normality after log-transformation. Thus, we used the Scheirer–Ray–Hare extension of the Kruskal–Wallis analysis of variance to account for multiple comparisons. The data were tested for differences between size (small and large) and treatment groups (control and OA) as well as for the interaction of the two groups. We used R to run non-parametric statistics. Results were considered significant if $P<0.05$.

RESULTS
Table 1 shows each breed we isolated cells from, as well as adult body mass and mean breed lifespan. We sampled a total of 114 dogs.

Quantifying lipids in fibroblast cell extracts
Collectively, cells from all dogs treated with OA had a higher double bond index overall compared with controls ($P<0.001$). Table 2 shows these collective changes in fatty acid composition between treatment groups, and a breed-by-breed breakdown of fatty acid composition changes in response to treatment is presented in Table S1. This difference was primarily driven by more MUFAs ($P<0.001$) and fewer saturated fatty acids ($P<0.001$) in the OA group, which offset the decrease in PUFAs in the OA group ($P<0.001$). Because of this decrease in PUFAs, especially ones with high double bond content such as DHA and arachidonic acid, the OA treatment had a lower peroxidizability index ($P=0.014$). We did not find a significant difference in any lipid variables between large and small breeds, nor did we find any significant correlations between average lifespan of each breed (data from Jimenez, 2016) and any lipid variable. Within individuals in both treatments, we found that as average fatty acid chain length increased, double bond index, peroxidizabilty and the percentage of MUFAs and PUFAs increased, whereas the percentage of saturated fatty acids decreased ($P<0.001$ for all).

OCR in fibroblast cells
When measuring the effects of body size (small breed and large breed), treatment (control and OA) and the interaction of size and treatment on basal OCR, we found that large breed puppies had a higher basal OCR than small breed puppies (size: $H=6.6$, $P=0.001$; Table 3). We found no differences between treatments, nor did we find a significant interaction between treatment and body size. When measuring the effects of the same variables on maximal respiration, we found that fibroblasts from the OA treatment had a significantly lower maximal respiration rate than controls ($H=3.8$, $P=0.051$; Fig. 1A), but no differences were found between sizes and there was no interaction (Table 3). Small breed OA-treated cells showed a decrease in spare respiratory capacity, indicating a smaller difference between basal and maximal OCR in this group ($H=6.6$, $P=0.01$; Fig. 1B). However, we found no differences between size groups or the interaction between size and treatment (Table 3). With respect to ATP coupling, fibroblasts from large breed puppies had a significantly higher ATP-coupled respiration ($H=9.3$, $P=0.002$; Table 3). However, there were no significant differences between treatments and no interactions. We also found no differences between size, treatments or interaction effects in proton leak. In line with their higher levels of ATP-coupled respiration, fibroblasts from large breeds also showed marginal significance for a higher coupling efficiency compared with those from small breeds ($H=3.6$, $P=0.059$; Fig. 1C). Additionally, OA-treated cells had a

Table 3. Mean±s.e.m. results for cellular metabolism and oxidative stress parameters between control and treated cells

Parameter	Size	Treatment	Mean±s.e.m.	Treatment	Mean±s.e.m.
Basal OCR (pmol min^{-1} per 20,000 cells)	Large	Control	239.56±24.09	OA	196.02±21.39
Basal OCR (pmol min^{-1} per 20,000 cells)	Small	Control	195.80±40.22	OA	178.40±29.15
Proton leak (mol min^{-1} per 20,000 cells)	Large	Control	72.33±7.33	OA	66.89±7.24
Proton leak (pmol min^{-1} per 20,000 cells)	Small	Control	68.23±13.94	OA	77.23±13.64
ATP-coupled respiration (pmol min^{-1} per 20,000 cells)	Large	Control	167.23±18.63	OA	130.10±15.13
ATP-coupled respiration (pmol min^{-1} per 20,000 cells)	Small	Control	127.32±28.21	OA	103.09±18.64
GSH (fluorescence per 20,000 cells)	Large	Control	34,883.24±5477.71	OA	22,489.51±3807.21
GSH (fluorescence per 20,000 cells)	Small	Control	43,345.24±10,531.52	OA	34,760.70±8743.65
ROS production (fluorescence per 20,000 cells)	Large	Control	29,732.47±4815.45	OA	23,407.39±2242.45
ROS production (fluorescence per 20,000 cells)	Small	Control	21,144.09±3550.62	OA	23,260.78±5301.86
LPO damage (fluorescence per 20,000 cells)	Large	Control	1.76±0.20	OA	1.76±0.22
LPO damage (fluorescence per 20,000 cells)	Small	Control	2.13±0.43	OA	2.04±0.36

Significant results can be found in Fig. 1. OCR, oxygen consumption rate; GSH, reduced glutathione; ROS, reactive oxygen species; LPO, lipid peroxidation.
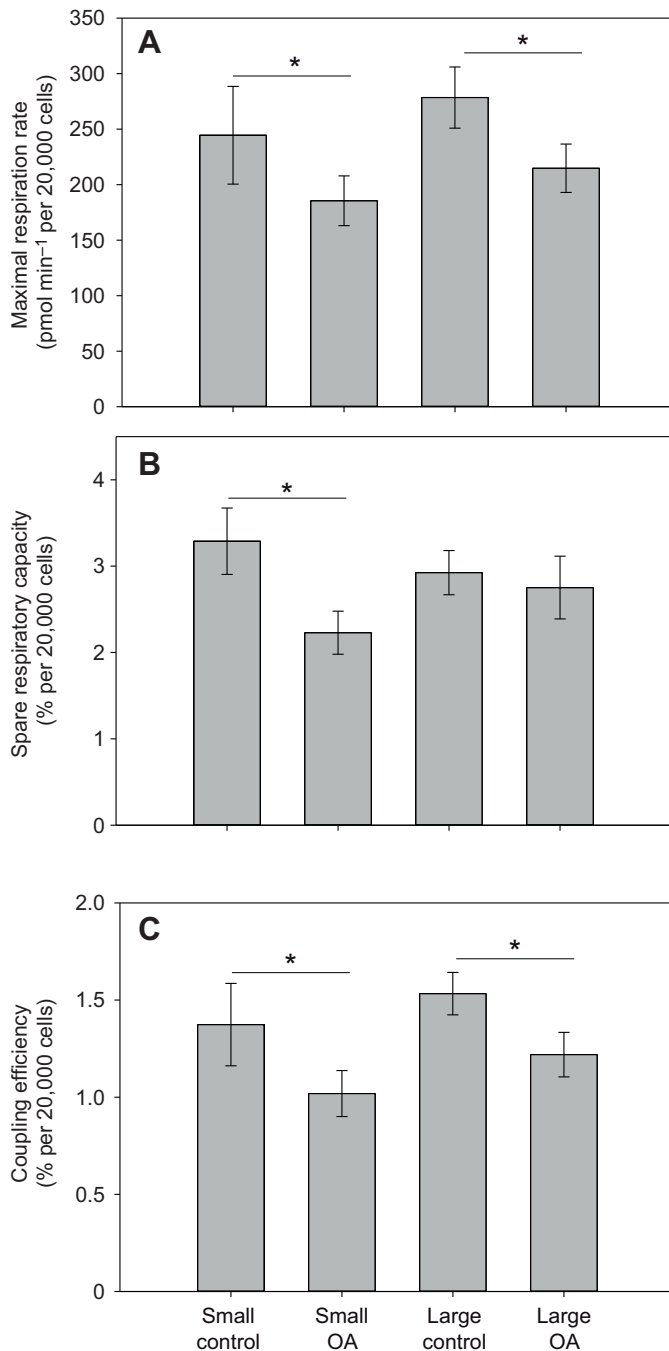
Fig. 1. Aerobic cellular metabolic rate in fibroblast cells. (A) Maximal respiration showed a marginally significant difference between treatment groups, but no differences were found between dog sizes. (B) Spare respiratory capacity showed significant differences between treatment groups; however, there were no differences between size groups. (C) Coupling efficiency showed a marginally significant difference between sizes and a significant difference between treatments. Asterisks indicate significant differences. Samples sizes can be found in Table 1.

lower coupling efficiency than control cells (H=10.1, P=0.002; Fig. 1C), but we found no interaction between body size and treatment. All results can be found in Table S2.

Oxidative stress measurements in fibroblast cells

ROS production, LPO damage and GSH showed no differences in size, treatment or an interaction (Table 3; Table S2).

DISCUSSION

Many studies have tracked the correlation between levels of membrane unsaturation, body size and lifespan; however, direct measurement of the oxidative stress system and cellular metabolism following cell membrane manipulation is lacking (Pamplona et al., 2000; Hulbert et al., 2005). We have directly tested the membrane as a pacemaker hypothesis of metabolism by comparing components of cellular metabolism and membrane fatty acid composition in fibroblast cells of dogs of different body sizes and lifespans. Additionally, we altered membrane fatty acid composition in these cells and measured subsequent changes in metabolic parameters. Finally, we indirectly tested the membrane pacemaker hypothesis of aging by assessing oxidative stress as a function of membrane fatty acid composition. We found that small dogs demonstrated lower basal cellular oxygen consumption rates and reduced ATP coupling efficiency compared with large dogs, but we found no differences in membrane fatty acid composition between these size classes. We also found that cells supplemented with OA had lower maximal respiration and reduced coupling efficiency compared with controls in small and large breed dogs, and that spare respiratory capacity decreased in OA-treated cells in small breed dogs, but not large breed dogs. These measurements may be linked to membrane lipid properties, as the OA group had more MUFAs and fewer PUFAs. These findings demonstrate that increasing the monounsaturation of dog membranes may alter cellular phenotypic traits that may be linked to their lifespan.

The negative correlation between body size and lifespan in dogs has been attributed to faster rates of aging in large dogs (Kraus et al., 2013; Jimenez, 2016), and the differences in various measures of oxygen consumption that we found here suggest a metabolic mechanism for these different rates of aging, in line with previous studies (Jimenez, 2016; Jimenez et al., 2018). The high ATP coupling efficiency we observed in fibroblasts from large dogs allows them to maximize energy efficiency and dedicate more energy toward growth, reproduction and external work (Rolfe and Brown, 1997). Because our cells were isolated from puppies, it is likely that the increased efficiency largely contributes to growth. Indeed, puppies have demonstrated lower proton leak than older dogs, indicating that a high degree of ATP coupling is important during growth (Jimenez et al., 2018). Furthermore, deliberate uncoupling of ATP synthesis has been shown to impair growth in other vertebrates (Bolser et al., 2018). Thus, increased coupling efficiency in the cells of large dogs may aid them in attaining larger body size. However, increased ATP coupling efficiency may also exert a metabolic cost on organisms. In general, a high degree of coupling efficiency is associated with an increase in mitochondrial membrane potential as more protons collect in the intermembrane space of the mitochondria, and this increased membrane potential is associated with greater production of ROS (Korshunov et al., 1997; Salin et al., 2018). Therefore, the enhanced degree of ATP coupling efficiency we observed in fibroblasts from large dogs may result in a higher degree of ROS production than in smaller dogs. Although we did not detect higher amounts of ROS or oxidative damage in large dogs, a multitude of factors may account for this apparent discrepancy, as discussed below.

Despite the lower basal OCR and lower ATP coupling efficiency in small dog breeds compared with large dog breeds (here and Jimenez et al., 2018), we did not find differences in membrane fatty acid chain composition between large and small dogs. These results are in contrast with previous correlations between metabolic rate and lipid unsaturation, in which high numbers of double bonds and PUFAs are associated with high proton leak and increased

transmembrane ion pumping, leading to elevated metabolic rates (Brookes et al., 1998; Hulbert and Else, 1999; Pamplona et al., 1999). The discrepancies between our results and previous studies may be attributed to a variety of factors. First, because we measured the lipid composition of all membranes and did not separate mitochondrial and plasma membranes, it is possible that contrasting fatty acid composition between the mitochondrial membrane and the plasma membrane offset such that we detected no difference in lipid composition between size classes (Calhoon et al., 2015). Indeed, our metabolic measurements support this assertion, as the high degree of ATP coupling in large dogs suggests a relatively impermeable inner mitochondrial membrane with fewer double bonds, whereas the high basal OCR overall suggests a more fluid, permeable plasma membrane with lots of double bonds and a high degree of transmembrane ion pumping. Follow-up studies that isolate the mitochondrial and plasma membrane prior to analysis could test this assertion. An additional explanation for the discrepancy between our metabolic measurements and fatty acid composition is that the effect of fatty acid tails on membrane permeability is often influenced by the phospholipid head groups associated with these tails. For example, certain n-3 PUFAs exhibit different effects on membrane structure when incorporated into phosphotidylcholines as opposed to phosphotidylethanolamines (Shaikh et al., 2015). Thus, measuring phospholipid content would add more insight into the relationship between membrane lipid composition and cellular metabolic rates in large and small dogs. Additionally, induced proton leak from uncoupling proteins (UCPs) also reduces ATP coupling efficiency (Brookes, 2005; Mori et al., 2008; Mailloux and Harper, 2012), and it is thus possible that small dogs have more active UCPs than large dogs. Lastly, our comparison is intraspecific whereas previous comparisons of membrane composition and body size and lifespan have focused in interspecies correlations (Hulbert et al., 2007).

In addition to the differences in coupling efficiency we found when comparing small and large dog breeds, we also found that treatment with OA decreases coupling efficiency in both small and large breeds. Here, differences in fatty acid composition between treatment and control groups suggest that coupling efficiency may be attributed in part to differences in lipids and attendant protein activities that increase mitochondrial membrane permeability in OA-treated cells. Because our OA cells had fewer PUFAs with high numbers of double bonds than controls, a high mitochondrial membrane permeability seems counterintuitive. However, membrane fluidity is most influenced by the addition of the first two double bonds to a saturated lipid chain and each additional double bond has less effect on overall membrane fluidity (Brenner, 1984; Pamplona et al., 2002). Therefore, because the OA cells had more double bonds overall than control cells, they may be able to exhibit greater mitochondrial membrane fluidity despite a lack of highly unsaturated PUFAs. Furthermore, the MUFA that increased the most in OA cells relative to controls was OA, and OA disproportionately increases membrane fluidity relative to its chain length and level of unsaturation (Epand et al., 1991). Previous studies further demonstrate the importance of MUFAs in determining membrane fluidity and influencing metabolic parameters. For example, decreased efficiency of ATP synthesis has also been found in rats with greater amounts of MUFAs and reduced PUFAs in mitochondrial membranes (Piquet et al., 2004). Additionally, whereas some studies experimentally manipulating the concentration of n-3 PUFAs in mitochondrial membranes have found mitochondrial respiration to not change (Lemieux et al., 2008), decrease (Yamaoka et al., 1988) or increase (McMillin et al.,

1992), these studies exhibited different patterns in MUFA concentration with respect to PUFA concentration. Furthermore, none of these studies exhibited the large increase in MUFA paired with a large decrease in saturated fatty acids that we observed in the OA-incubated cells compared with controls. Overall, our data suggest that MUFA concentration may play a large role in determining cell membrane properties and thus controlling metabolic parameters.

The high degree of ATP coupling in cells from large dogs and in control cells versus cells from small dogs and OA-treated cells, respectively, combined with a higher peroxidizability in control cells suggest greater amounts of ROS production and oxidative damage in these cells. However, we found no differences in ROS production, LPO damage and GSH concentration for our cells. Overall, studies correlating cellular membrane fatty acid composition with ROS production have produced mixed results, with ROS production sometimes increasing as unsaturated fatty acids within tissues increase (Pamplona et al., 2000), and sometimes decreasing or remaining unchanged (Ramsey et al., 2005; Hagopian et al., 2010). There are at least four reasons why our results and the results of other studies are inconsistent in their correlations between metabolic parameters, lipid membrane composition and ROS production. First, enzymatic antioxidants such as SOD and CAT are sometimes upregulated in response to enhanced ATP coupling efficiency, and are able to quench excess ROS (Brookes, 2005). Second, whereas the mechanistic detail has not been elucidated, there seems to be strong support for the idea that UCP2 and UCP3 (found in fibroblasts) play a role in protection from ROS damage; thus, changes in the activity or amount of UCPs could mitigate ROS damage (Echtay and Brand, 2007; Mori et al., 2008). Third, damaged PUFAs on membrane phospholipids are very quickly replaced by undamaged PUFAs by deacylation/reacylation remodeling to repair LPO damage (Hulbert et al., 2014). Finally, our cells were isolated from medically discarded tissues from puppies, and therefore may have been less susceptible to LPO damage, as during senescence membranes become more rigid and the process of LPO damage becomes accentuated (Hulbert, 2005).

It has been shown that ROS production and LPO damage increase as a function of the degree of unsaturation of the fatty acid substrates in tissues (Pamplona et al., 2000). In a cross-sectional study, mice were fed calorie-restricted diets with differing fatty acids, the group of mice that were fed the lower polyunsaturated diet demonstrated a significant reduction of ROS production through complex III (López-Domínguez et al., 2015). In rats consuming fish oil, liver mitochondrial H_2O_2 production either decreased or remained unchanged when there was no increase in mitochondrial oxidative damage (Ramsey et al., 2005; Hagopian et al., 2010). In rats chronically fed diets with different fatty acid unsaturation, the double bond content of liver and brain was successfully manipulated. LPO damage product malondialdehyde and mitochondrial DNA oxidative damage significantly increased in rats fed an unsaturated diet compared with those fed control diets in both tissues (Pamplona et al., 2004). Thus, it seems that LPO damage can increase, decrease or stay the same during lipid membrane manipulations.

It is noteworthy to point out that large breeds show a decrease in maximal respiratory capacity in OA-treated cells with no change in spare respiratory capacity. Spare respiratory capacity allows cells to meet increased energy demands under conditions of severe stress, including detoxification of ROS and repairing cellular damage (Hill et al., 2009). Therefore, our results suggest that treatment with OA may especially benefit large dog breeds by reducing maximal

respiration, which is associated with longer lifespans (Hulbert et al., 2007), while maintaining spare respiratory capacity to respond to cellular stress.

In conclusion, we have found that metabolic parameters in dog fibroblasts vary between large and small dogs, and that these parameters may be altered by changing membrane fatty acid composition. Cells from small dogs exhibited lower ATP coupling efficiency than cells from large dogs, and reduced ATP coupling efficiency is often associated with reduced ROS production (Brookes, 2005; Salin et al., 2018). Although we did not find differences in membrane fatty acid composition between small and large breed dogs, we found that when we experimentally altered fatty acid composition such that cell membranes contained more MUFAs and fewer PUFAs, we were able to reduce ATP coupling efficiency and reduce maximal respiration. Taken together, our results suggest that increasing the monounsaturation of fatty acids in dog cell membranes may alter metabolic function in a way that is associated with greater longevity. Although we found some inconsistencies between variables in our data, separation of lipid membranes and direct measurements of membrane fluidity, phospholipid composition and UCP activity, among other variables, may enable us to address these inconsistencies in future studies (Calhoon et al., 2015). Such studies would allow us to build a cohesive model of the role of cellular membranes as pacemakers of metabolism and longevity.

References
Abbott, S. K., Else, P. L., Atkins, T. A. and Hulbert, A. J. (2012). Fatty acid composition of membrane bilayers: importance of diet polyunsaturated fat balance. *Biochim. Biophys. Acta Biomembr.* **1818**, 1309-1317. doi:10.1016/j.bbamem.2012.01.011

Bolser, D. G., Dreier, D. A., Li, E., Kroll, K. J., Martyniuk, C. J. and Denslow, N. D. (2018). Toward an adverse outcome pathway for impaired growth: mitochondrial dysfunction impairs growth in early life stages of the fathead minnow (Pimephales promelas). *Comp. Biochem. Physiol. C Toxicol. Pharmacol.* **209**, 46-53. doi:10.1016/j.cbpc.2018.03.009

Bligh, E. G. and Dyer, W. J. (1959). A rapid method of total lipid extraction and purification. *Can. J. Biochem. Physiol.* **37**, 911-917. doi:10.1139/y59-099

Brand, M. D. and Nicholls, D. G. (2011). Assessing mitochondrial dysfunction in cells. *Biochem. J.* **435**, 297-312. doi:10.1042/BJ20110162

Brenner, R. (1984). Effect of unsaturated acids on membrane structure and enzyme kinetics. *Prog. Lipid Res.* **23**, 69-96. doi:10.1016/0163-7827(84)90008-0

Brookes, P. S., (2005). Mitochondrial H+ leak and ROS generation: an odd couple. *Free Radic. Biol. Med.* **38**, 12-23. doi:10.1016/j.freeradbiomed.2004.10.016

Brookes, P. S., Buckingham, J. A., Tenreiro, A. M., Hulbert, A. J., and Brand, M. D. (1998). The proton permeability of the inner membrane of liver mitochondria from ectothermic and endothermic vertebrates and from obese rats: correlations with standard metabolic rate and phospholipid fatty acid composition. *Comp. Biochem. Physiol. B.* **119**, 325-334. doi:10.1016/s0305-0491(97)00357-x

Calhoon, E. A., Jimenez, A. G., Harper, J. M., Jurkowitz, M. S. and Williams, J. B. (2014). Linkages between mitochondrial lipids and life history in temperate and tropical birds. *Physiol. Biochem. Zool.* **87**, 265-275. doi:10.1086/674696

Calhoon, E. A., Ro, J. and Williams, J. B. (2015). Perspectives on the membrane fatty acid unsaturation/pacemaker hypotheses of metabolism and aging. *Chem. Phys. Lipids* **191**, 48-60. doi:10.1016/j.chemphyslip.2015.08.008

Choi, H., Yang, Z. and Weisshaar, J. C. (2015). Single-cell, real-time detection of oxidative stress induced in Escherichia coli by the antimicrobial peptide CM15. *Proc. Natl. Acad. Sci. USA* **112**, E303-E310. doi:10.1073/pnas.1417703112

Couture, P. and Hulbert, A. J. (1995a). Membrane fatty acid composition of tissues is related to body mass of mammals. *J. Membr. Biol.* **148**, 27-39. doi:10.1007/BF00234153

Couture, P. and Hulbert, A. J. (1995b). Relationship between body mass, tissue metabolic rate, and sodium pump activity in mammalian liver and kidney. *Am. J. Physiol. Regul. Integr. Comp. Physiol.* **268**, R641-R650. doi:10.1152/ajpregu.1995.268.3.R641

Cury-Boaventura, M. F., Gorjão, R., De Lima, T. M., Newsholme, P. and Curi, R. (2006). Comparative toxicity of oleic and linoleic acid on human lymphocytes. *Life Sci.* **78**, 1448-1456. doi:10.1016/j.lfs.2005.07.038

Dezest, M., Chavatte, L., Bourdens, M., Quinton, D., Camus, M., Garrigues, L., Descargues, P., Arbault, S., Burlet-Schiltz, O., Casteilla, L. et al. (2017). Mechanistic insights into the impact of Cold Atmospheric Pressure Plasma on human epithelial cell lines. *Sci. Rep.* **7**, 41163. doi:10.1038/srep41163

Divakaruni, A. S., Paradyse, A., Ferrick, D. A., Murphy, A. N. Jastroch, M. (2014). Analysis and interpretation of microplate-based oxygen consumption and pH data. *Methods Enzymol.* **547**, 309-354. doi:10.1016/B978-0-12-801415-8.00016-3

Echtay, K. S. and Brand, M. D. (2007). 4-hydroxy-2-nonenal and uncoupling proteins: an approach for regulation of mitochondrial ROS production. *Redox Rep.* **12**, 26-29. doi:10.1179/135100007X162158

Epand, R. M., Epand, R. F., Ahmed, N. and Chen, R., (1991). Promotion of hexagonal phase formation and lipid mixing by fatty acids with varying degrees of unsaturation. *Chem. Phys. Lipids* **57**, 75-80. doi:10.1016/0009-3084(91)90051-c

Escribá, P. V., Sastre, M. and García-Sevilla, J. A. (1995). Disruption of cellular signaling pathways by daunomycin through destabilization of nonlamellar membrane structures. *Proc. Natl. Acad. Sci. USA* **92**, 7595-7599. doi:10.1073/pnas.92.16.7595

Gebhard, A. W., Jain, P., Nair, R. R., Emmons, M. F., Argilagos, R. F., Koomen, J. M., McLaughlin, M. L. and Hazlehurst, L. A. (2013). MTI101 (cyclized HYD1) binds a CD44 containing complex and induces necrotic cell death in multiple myeloma. *Mol. Cancer Ther.* **12**, 2446-2458. Doi:10.1158/1535-7163.MCT-13-0310

Gerenser, A. A., Neilson, A., Choi, S. W., Edman, U., Yadava, N, Oh, R. J., Ferrick, D. A., Nicholls, D. G., and Brand, M. D. (2009). Quantitative microplate-based respirometry with correction for oxygen diffusion. *Anal. Chem.* **81**, 6868-6878. doi:10.1021/ac900881z

Girelli, D., Lupo, A., Trevisan, M. T., Olivieri, O., Bernich, P., Zorzan, P., Bassi, A., Stanzial, A. M., Ferrari, S. and Corrocher, R. (1992). Red blood cell susceptibility to lipid peroxidation, membrane lipid composition, and antioxidant enzymes in continuous ambulatory peritoneal dialysis patients. *Perit. Dial. Int.* **12**, 205-210. doi:10.1177/089686089201200204

Glaser, M., Ferguson, K. A. and Vagelos, P. R. (1974). Manipulation of the phospholipid composition of tissue culture cells. *Proc. Natl. Acad. Sci. USA* **71**, 4072-4076. doi:10.1073/pnas.71.10.4072

Guillou, H., Zadravec, D., Martin, P. G. P. and Jacobsson, A. (2010). The key roles of elongases and desaturases in mammalian fatty acid metabolism: insights from transgenic mice. *Prog. Lipid Res.* **49**, 186-199. doi:10.1016/j.plipres.2009.12.002

Hagopian, K., Weber, K. L., Hwee, D. T., Van Eenennaam, A. L., López-Lluch, G., Villalba, J. M., Burón, I., Navas, P., German, J. B., Watkins, S. M. et al. (2010). Complex I-associated hydrogen peroxide production is decreased and electron transport chain enzyme activities are altered in n-3 enriched fat-1 mice. *PLoS ONE* **5**, e12696. doi:10.1371/journal.pone.0012696

Halliwell, B. and Gutteridge, J. M. (2015). *Free Radicals in Biology and Medicine.* USA: Oxford University Press.

Harman, D. (1956). Aging: A theory based on free radical and radiation chemistry. *J. Gerontol.* **11**, 298-300. doi:10.1093/geronj/11.3.298.

Harman, D. (1994). Free-radical theory of aging: increasing the functional life span. *Annals N.Y. Acad. Sci.* **717**, 1-15. doi:10.1111/j.1749-6632.1994.tb12069.x.

Hill, B. G., Dranka, B. P., Zou, L., Chatham, J. C. and Darley-Usmar, V. M. (2009). Importance of the bioenergetic reserve capacity in response to cardiomyocyte stress induced by 4-hydroxynonenal. *Biochem. J.* **424**, 99-107. doi:10.1042/BJ20090934

Hill, B. G., Benavides, G. A., Lancaster, J. R., , Jr, Ballinger, S., Dell'Italia, L., Zhnag, J. and Darley-Usmar, V. M. (2012). Integration of cellular bioenergetics with mitochondrial quality control and autophagy. *Biol. Chem.* **393**, 1485- 1512. doi:10.1515/hsz-2012-0198

Huang, Q., Sun, D., Hussain, M. Z., Liu, Y., Morozova-Roche, L. A. and Zhang, C. (2019). HEWL interacts with dissipated oleic acid micelles, and decreases oleic acid cytotoxicity. *PLoS ONE* **14**, e0212648. doi:10.1371/journal.pone.0212648

Hulbert, A. J. (2005). On the importance of fatty acid composition of membranes for aging. *J. Theor. Biol.* **234**, 277-288. doi:10.1016/j.jtbi.2004.11.024

Hulbert, A. J. and Else, P. L. (1999). Membranes as possible pacemakers of metabolism. *J. Theor. Biol.* **199**, 257-274. doi:10.1006/jtbi.1999.0955

Hulbert, A. J., Rana, T. and Couture, P. (2002). The acyl composition of mammalian phospholipids: an allometric analysis. *Comp. Biochem. Physiol. B Biochem. Mol. Biol.* **132**, 515-527. doi:10.1016/S1096-4959(02)00066-0

Hulbert, A. J., Turner, N., Storlien, L. H. and Else, P. L. (2005). Dietary fats and membrane function: implications for metabolism and disease. *Biol. Rev.* **80**, 155-169. doi:10.1017/s1464793104006578

Hulbert, A. J., Pamplona, R., Buffenstein, R. and Buttemer, W. A. (2007). Life and death: metabolic rate, membrane composition, and life span of animals. *Physiol. Rev.* **87**, 1175-1213. doi:10.1152/physrev.00047.2006

Hulbert, A. J., Kelly, M. A. and Abbott, S. K. (2014). Polyunsaturated fats, membrane lipids and animal longevity. *J. Comp. Physiol. B* **184**, 149-166. doi:10.1007/s00360-013-0786-8

Ichihara, K. and Fukubayashi, Y. (2010). Preparation of fatty acid methyl esters for gas-liquid chromatography. *J. Lipid Res.* **51**, 635-640. doi:10.1194/jlr.D001065

Jimenez, A. G. (2016). Physiological underpinnings in life-history trade-offs in man's most popular selection experiment: the dog. *J. Comp. Physiol. B* **186**, 813-827. doi:10.1007/s00360-016-1002-4

Jimenez, A. G., Winward, J., Beattie, U. and Cipolli, W. (2018). Cellular metabolism and oxidative stress as a possible determinant for longevity in small breed and large breed dogs. *PLoS ONE* **13**, e0195832. doi:10.1371/journal.pone.0195832

Korshunov, S. S., Skulachev, V. P. and Starkov, A. A. (1997). High protonic potential actuates a mechanism of production of reactive oxygen species in mitochondria. *FEBS Lett.* **416**, 15-18. doi:10.1016/S0014-5793(97)01159-9

Kraus C., Pavard S. and Promislow D. E. (2013). The size-life span trade-off decomposed: why large dogs die young. *Am. Natural.* **181**, 492-505. doi:10.1086/669665

Leirós, M., Alonso, E., Rateb, M. E., Houssen, W. E., Ebel, R., Jaspars, M., Alfonso, A. and Botana, L. M. (2014). Bromoalkaloids protect primary cortical neurons from induced oxidative stress. *ACS Chem. Neurosci.* **6**, 331-338. doi:10.1021/cn500258c

Lemieux, H., Blier, P. U. and Tardif, J.-C. (2008). Does membrane fatty acid composition modulate mitochondrial functions and their thermal sensitivities? *Comp. Biochem. Physiol. A Mol. Integr. Physiol.* **149**, 20-29. doi:10.1016/j.cbpa.2007.09.015

López-Domínguez, J. A., Ramsey, J. J., Tran, D., Imai, D. M., Koehne, A., Laing, S. T., Griffey, S. M., Kim, K., Taylor, S. L., Hagopian, K. et al. (2015). The influence of dietary fat source on life span in calorie restricted mice. *J. Gerontol. A Biomed. Sci. Med. Sci.* **70**, 1181-1188. doi:10.1093/gerona/glu177

Mailloux, R. J. and Harper, M. (2012). Mitochondrial proticity and ROS signaling: lessons from the uncoupling proteins. *Trends Endocrinol. Med.* **23**, 451-458. doi:10.1016/j.tem.2012.04.004

Mandavilli, B. S. and Janes, M. S. (2010). Detection of intracellular glutathione using ThiolTracker violet stain and fluorescence microscopy. *Curr. Protoc. Cytom.* **53**, 9.35.1-9.35.8. doi:10.1002/0471142956.cy0935s53

McMillin, J. B., Bick, R. J. and Benedict, C. R. (1992). Influence of dietary fish oil on mitochondrial function and response to ischemia. *Am. J. Physiol. Heart Circ. Physiol.* **263**, H1479-H1485. doi:10.1152/ajpheart.1992.263.5.H1479

Monaghan, P., Metcalfe, N. B. and Torres, R. (2009). Oxidative stress as a mediator of life history trade-offs: mechanisms, measurements and interpretation. *Ecol. Lett.* **12**, 75-92. doi:10.1111/j.1461-0248.2008.01258.x

Mori, S., Yoshizuka, N., Takizawa, M., Takema, Y., Murase, T., Tokimitsu, I. and Saito, M. (2008). Expression of uncoupling proteins in human skin and skin-derived cells. *J. Investig. Dermatol.* **128**, 1894-1900. doi:10.1038/jid.2008.20

Naudí, A., Jové, M., Ayala, V., Portero-Otín, M., Barja, G. and Pamplona, R. (2013). Membrane lipid unsaturation as physiological adaptation to animal longevity. *Front. Physiol.* **4**, 372. doi:10.3389/fphys.2013.00372

Pamplona, R., Prat, J., Cadenas, S., Rojas, C., Perez-Campo, R., Torres, M. L. and Barja, G. (1996). Low fatty acid unsaturation protects against lipid peroxidation in liver mitochondria from long-lived species: the pigeon and human case. *Mech. Ageing Dev.* **86**, 53-66. doi:10.1016/0047-6374(95)01673-2

Pamplona, R., Portero-Otin, M., Riba, D., Ruiz, C., Prat, J., Bellmunt, M. J. and Barja, G. (1998). Mitochondrial membrane peroxidizability index is inversely related to maximum lifespan in mammals. *J. Lipid Res.* **39**, 1989-1994.

Pamplona, R., Portero-Otín, M., Riba, D., Ledo, F., Gredilla, R., Herrero, A. and Barja, G. (1999). Heart fatty acid unsaturation and lipid peroxidation, and aging rate, are lower in the canary and the parakeet than in the mouse. *Aging Clin. Exp. Res.* **11**, 44-49. doi:10.1007/BF03399636

Pamplona, R., Portero-Otín, M., Riba, D., Requena, J. R., Thorpe, S. R., López-Torres, M. and Barja, G. (2000). Low fatty acid unsaturation: a mechanism for lowered lipoperoxidative modification of tissue proteins in mammalian species with long life spans. *J. Gerontol. A Biol. Sci. Med. Sci.* **55**, B286-B291. doi:10.1093/gerona/55.6.b286

Pamplona, R., Barja, G. and Portero-Otín, M. (2002). Membrane fatty acid unsaturation, protection against oxidative stress, and maximum life span: a homeoviscous-longevity adaptation? *Ann. N. Y. Acad. Sci.* **959**, 475-490. doi:10.1111/j.1749-6632.2002.tb02118.x

Pamplona, R., Portero-Otın, M., Sanz, A., Requena, J. and Barja, G. (2004). Modification of the longevity-related degree of fatty acid unsaturation modulates oxidative damage to proteins and mitochondrial DNA in liver and brain. *Exp. Gerontol.* **39**, 725-733. doi:10.1016/j.exger.2004.01.006

Pappas, A., Anthonavage, M. and Gordon, J. S. (2002). Metabolic fate and selective utilization of major fatty acids in human sebaceous gland. *J. Investig. Dermatol.* **118**, 164-171. doi:10.1046/j.0022-202x.2001.01612.x

Piquet, M. A., Roulet, M., Nogueira, V., Filippi, C., Sibille, B., Hourmand-Ollivier, I. and Leverve, X. M. (2004). Polyunsaturated fatty acid deficiency reverses effects of alcohol on mitochondrial energy metabolism. *J. Hepatol.* **41**, 721-729. doi:10.1016/j.jhep.2004.07.002

Portero-Otín, M., Bellumunt, M. J., Ruiz, M. C., Barja, G. and Pamplona, R. (2001). Correlation of fatty acid unsaturation of the major liver mitochondrial phospholipid classes in mammals to their maximum life span potential. *Lipids* **36**, 491-498. doi:10.1007/s11745-001-0748-y

Ramsey, J. J., Harper, M.-E., Humble, S. J., Koomson, E. K., Ram, J. J., Bevilacqua, L. and Hagopian, K. (2005). Influence of mitochondrial membrane fatty acid composition on proton leak and H2O2 production in liver. *Comp. Biochem. Physiol. B Biochem. Mol. Biol.* **140**, 99-108. doi:10.1016/j.cbpc.2004.09.016

Roberts, J. S., Atanasova, K. R., Lee, J., Diamond, G., Deguzman, J., Hee Choi, C. and Yilmaz, Ö. (2017). Opportunistic pathogen Porphyromonas gingivalis modulates danger signal ATP-mediated antibacterial NOX2 pathways in primary epithelial cells. *Front. Cell. Infect. Microbiol.* **7**, 291. doi:10.3389/fcimb.2017.00291

Rolfe, D. F. and Brown, G. C. (1997). Cellular energy utilization and molecular origin of standard metabolic rate in mammals. *Physiol. Rev.* **77**, 731-758. doi:10.1152/physrev.1997.77.3.731

Salin, K., Villasevil, E. M., Anderson, G. J., Auer, S. K., Selman, C., Hartley, R. C., Mullen, W., Chinopoulos, C. and Metcalfe, N. B. (2018). Decreased mitochondrial metabolic requirements in fasting animals carry an oxidative cost. *Funct. Ecol.* **32**, 2149-2157. doi:10.1111/1365-2435.13125

Shaikh, S. R., Kinnun, J. J., Leng, X., Williams, J. A. and Wassall, S. R. (2015). How polyunsaturated fatty acids modify molecular organization in membranes: insight from NMR studies of model systems. *Biochim. Biophys. Acta* **1848**, 211-219. doi:10.1016/j.bbamem.2014.04.020

Speakman, J. R. (2005). Correlations between physiology and lifespan–two widely ignored problems with comparative studies. *Aging Cell* **4**, 167-175. doi:10.1111/j.1474-9726.2005.00162.x

Spector, A. A. and Yorek, M. A. (1985). Membrane lipid composition and cellular function. *J. Lipid Res.* **26**, 1015-1035.

Templeton, G. F. (2011). A two-step approach for transforming continuous variables to normal: implications and recommendations for IS research. *Commun. Assoc. Info. Syst.* **28**, 4. doi:10.17705/1cais.02804

Thannickal, V. J. and Fanburg, B. L. (2000). Reactive oxygen species in cell signaling. *Am. J. Physiol. Lung Cell. Mol. Physiol.* **279**, L1005-L1028. doi:10.1152/ajplung.2000.279.6.L1005

Turner, N., Else, P. L. and Hulbert, A. J. (2003). Docosahexaenoic acid (DHA) content of membranes determines molecular activity of the sodium pump: implications for disease states and metabolism. *Naturwissenschaften* **90**, 521-523. doi:10.1007/s00114-003-0470-z

Turner, N., Haga, K. L., Hulbert, A. J. and Else, P. L. (2005). Relationship between body size, Na$^+$-K$^+$-ATPase activity, and membrane lipid composition in mammal and bird kidney. *Am. J. Physiol. Regul. Integr. Comp. Physiol.* **288**, R301-R310. doi:10.1152/ajpregu.00297.2004

Valencak, T. G. and Ruf, T. (2011). Feeding into old age: long-term effects of dietary fatty acid supplementation on tissue composition and life span in mice. *J. Comp. Physiol. B* **181**, 289-298. doi:10.1007/s00360-010-0520-8

Yamamoto, Y., Fujisawa, A., Hara, A. and Dunlap, W. C. (2001). An unusual vitamin E constituent (α-tocomonoenol) provides enhanced antioxidant protection in marine organisms adapted to cold-water environments. *Proc. Natl. Acad. Sci. USA* **98**, 13144-13148. doi:10.1073/pnas.241024298

Yamaoka, S., Urade, R. and Kito, M. (1988). Mitochondrial function in rats is affected by modification of membrane phospholipids with dietary sardine oil. *J. Nutr.* **118**, 290-296. doi:10.1093/jn/118.3.290

Zou, Y., and Yu, H. (2018). Improving the analysis of 37 fatty acid methyl esters using three types of capillary GC columns. *Agilent Technologies Application Note.* Publication Number 5991-8706EN.